New Journal of Physics
The open-access journal for physics

Asymmetric Coulomb blockade and Kondo temperature of single-molecule transistors

Florian Elste[1] **and Felix von Oppen**
Institut für Theoretische Physik, Freie Universität Berlin, Arnimallee 14, D-14195 Berlin, Germany
E-mail: felste@physik.fu-berlin.de

New Journal of Physics **10** (2008) 065021 (8pp)
Received 3 April 2008
Published 30 June 2008
Online at http://www.njp.org/
doi:10.1088/1367-2630/10/6/065021

Abstract. Recent experiments on single-molecule transistors made of cobalt complexes exhibited anomalously weak gate voltage dependence of the Kondo temperature accompanied by a strong asymmetry in the Coulomb blockade peaks. We show that these observations can both be explained by strong electron–vibron interactions when including *anharmonicities* of the molecular potential surfaces. The strong electron–vibron interactions may originate from a tendency of the cobalt complexes toward Jahn–Teller distortion.

Contents

1. Introduction

The occurrence of the Kondo effect in transport through artificial nanostructures such as quantum dots was predicted long ago [1, 2]. Its experimental observation [3] has generated considerable interest in recent years, leading to numerous experimental and theoretical works [4]–[8] (for a review, see [9]). An important question addressed by these works is the fate of the Kondo effect out of equilibrium due to the presence of a bias voltage [10]–[12].

[1] Author to whom any correspondence should be addressed.

In quantum dots a quantitative description of the build-up of Kondo correlations is possible in terms of the single-impurity Anderson model,

$$H_0 = \sum_{\alpha k\sigma} \varepsilon_{\alpha k} c^\dagger_{\alpha k\sigma} c_{\alpha k\sigma} + \epsilon_{\rm d}(n_\uparrow + n_\downarrow) + U n_\uparrow n_\downarrow + \sum_{\alpha k\sigma} \left[t_{\alpha k} c^\dagger_{\alpha k\sigma} d_\sigma + t^*_{\alpha k} d^\dagger_\sigma c_{\alpha k\sigma} \right], \quad (1)$$

where $d^\dagger_\sigma (c^\dagger_{\alpha k\sigma})$ creates an electron with energy $\epsilon_{\rm d}$ (with energy $\varepsilon_{\alpha k}$ and momentum k in lead α) and spin σ on the dot (in the reservoir), U is the local Coulomb repulsion of the electrons and $n_\sigma = d^\dagger_\sigma d_\sigma$. For single occupation of the localized level, the exchange between the spin of the localized electron and the spin of the conduction electrons is obtained from a Schrieffer–Wolff transformation and yields

$$J = 2t^2 \left(\frac{1}{\epsilon_{\rm d}} - \frac{1}{\epsilon_{\rm d} + U} \right), \quad (2)$$

for $\varepsilon_{\alpha k} \ll \epsilon_{\rm d}, U$ and $t_{\alpha k} \approx t$. In single-electron transistors the onsite energy $\epsilon_{\rm d}$ can effectively be shifted by applying an additional gate voltage $V_{\rm g}$. Employing poor man's scaling, one can derive an expression for the dependence of the Kondo temperature $T_{\rm K} \sim {\rm e}^{-1/\nu J}$ on gate voltage,

$$T_{\rm K} = \frac{\sqrt{\Gamma U}}{2} {\rm e}^{\pi \epsilon_{\rm d}(U+\epsilon_{\rm d})/\Gamma U}, \quad (3)$$

which provides an excellent description of experimental observations in quantum dots [5]. (Here, Γ denotes the coupling to the leads and ν denotes the local density of states in the leads.)

Surprisingly, recent experiments by Yu *et al* [13] have revealed that equation (3) does not work in certain single-molecule junctions, composed of the transition metal complex [di-(di-pyridyl-pyrrolato)cobalt]. Instead the gate dependence of the Kondo temperature is found to be much weaker. Interestingly, this observation is coupled to a strongly asymmetric Coulomb blockade: measurements of the differential conductance as a function of bias and gate voltage show Coulomb diamonds with significantly different peak intensities at the two opposite sides of the charge degeneracy point [13]–[16]. The persistence of these unusual features in different single-molecule devices suggests that their explanation can be ascribed to molecule-specific degrees of freedom such as molecular vibrations. Indeed, it is natural to expect that the octahedral cobalt complexes exhibit a tendency toward Jahn–Teller distortions, which may induce a strong electron–vibron interaction.

In two recent works, Balseiro *et al* [17] suggested that strong electron–vibron interactions could explain the weak dependence $T_{\rm K}(V_{\rm g})$. The principal idea is that for strong electron–vibron coupling the dominant contribution to the kinetic exchange stems from virtual charge fluctuations involving higher-excited vibrational states. In this case, the energy denominators in equation (2) are modified to include the vibrational excitation energy of the intermediate states for which the Franck–Condon overlap with the vibrational ground state is maximal. As a result the dependence of J, and hence $T_{\rm K}$, on the gate voltage is suppressed as compared to the situation of weak or no electron–vibron coupling. These authors also show numerical results, based on the numerical renormalization group technique, which are consistent with the asymmetric Coulomb blockade.

The purpose of the present paper is to point out that strong electron–vibron coupling may also naturally account for the observation of a pronounced asymmetry of the Coulomb blockade diamonds in an *alternative* manner. Indeed, strong electron–vibron coupling implies that tunneling of electrons onto or off the molecule is accompanied by significant molecular deformations. This suggests that one should go beyond the common assumption of harmonic

vibrations by including *anharmonicities* of the molecular potential surfaces. Our central result is that these anharmonicities can lead to strongly asymmetric Coulomb blockade diamonds.

We discuss our model and methods in section 2. Our principal results are contained in section 3. We summarize and conclude in section 4.

2. Model and methods

Our results are based on a model which considers a molecule weakly coupled to two metallic leads. We assume transport to be dominated by a single molecular level with onsite energy ϵ_{d} and local Coulomb repulsion U. In addition to H_0, the full Hamiltonian contains a vibrational contribution,

$$H = H_0 + \frac{P^2}{2\mu} + V_n(X), \tag{4}$$

describing the kinetic and potential energies for the collective vibrational mode X. P and μ denote the momentum and the reduced mass of the nuclear motion. Due to the electron–vibron coupling, the potential energy $V_n(X)$ depends on the molecular charge state n.

This dependence is included through a global shift of the potential surface, $V_n(X) = \sum_n v(X - \sqrt{2}n\lambda l)|n\rangle\langle n|$, where $|n\rangle$ denotes the electronic state with charge n, λ the dimensionless electron–vibron coupling strength and $l = (\hbar/\mu\omega_0)^{1/2}$ the oscillator length. The anharmonic shape $v(X)$ of the potential surface is modeled by a Morse potential [18],

$$v(X) = D\left[\mathrm{e}^{-2\beta X} - 2\mathrm{e}^{-\beta X}\right]. \tag{5}$$

The curvature of $v(X)$ at the minimum is given by $\omega_0 = \beta^2\sqrt{2D}/\mu$. The energies of bound states of the Morse oscillator are given by $E_q = \hbar\omega_0(q + 1/2) - \chi\hbar\omega_0(q + 1/2)^2$, cf [18]. The parameter χ determines the asymmetry of the Morse potential in comparison with the harmonic potential and the number of bound states which is given by $j = \lfloor(1/\chi - 1)/2\rfloor$. Here, half-brackets are used to denote the integer part.

The occupation probabilities P_q^n of the molecular eigenstates $|n, q\rangle$ with electronic occupancy n and vibrational quantum number q are obtained by solving rate equations, $\mathrm{d}P_q^n/\mathrm{d}t = \sum_{n'q'}(P_{q'}^{n'}W_{q'\to q}^{n'\to n} - P_q^n W_{q\to q'}^{n\to n'}) - \frac{1}{\tau}(P_q^n - P^{\mathrm{eq}}\sum_{q'}P_{q'}^n)$ [19]–[21]. Here $W_{q\to q'}^{n'\to n}$ is the rate for a transition from state $|n, q\rangle$ to $|n', q'\rangle$. The last term describes the fact that the vibrations relax toward the equilibrium distribution $P_q^{\mathrm{eq}} = \mathrm{e}^{-\hbar\omega_0/kT}[1 - \mathrm{e}^{-\hbar\omega_0/kT}]$ on the phenomenological timescale τ. Here, we always assume fast vibrational relaxation, i.e. $\tau \approx 0$[2].

Second-order perturbation theory in the tunneling Hamiltonian yields a *golden-rule* expression for the transition rates,

$$W_{q\to q',\alpha}^{n\to n'} = 2\pi t^2 \nu \left|M_{q\to q'}^{n\to n'}\right|^2 \left\{f(-\Delta_{nn'}^c + (q'-q)\hbar\omega_0 - \mu_\alpha) + [1 - f(\Delta_{nn'}^c + (q-q')\hbar\omega_0 - \mu_\alpha)]\right\}, \tag{6}$$

where f denotes the Dirac–Fermi function, ν the local density of states in the leads, μ_α the chemical potential of lead α, $\Delta_{nn'}^c \equiv \epsilon_d(n'-n) + Un'(n'-1)/2 - Un(n-1)/2$ and $M_{q\to q'}^{n\to n'} = \int_{-\infty}^{\infty}\mathrm{d}x\,\phi_{n,q}^*(x)\phi_{n',q'}(x)$ the Franck–Condon matrix element of two eigenfunctions of

[2] Effects of nonequilibrium for anharmonic molecular vibrations have been considered in [22].

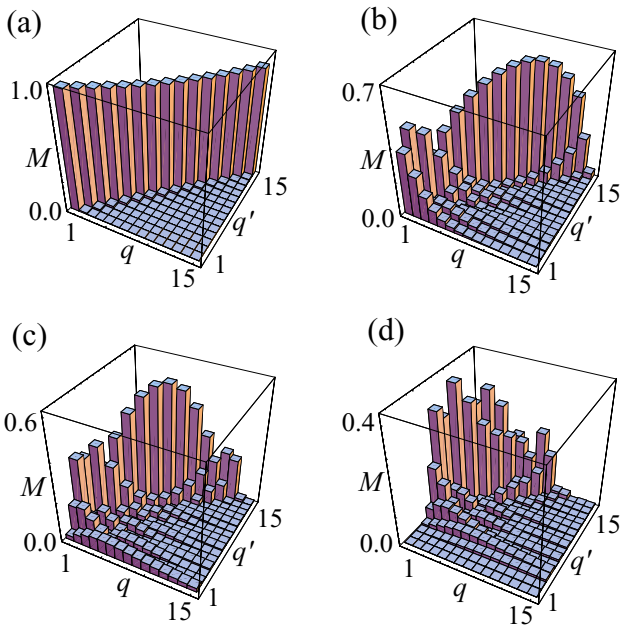

Figure 1. Franck–Condon matrix elements, $M^{0\to 1}_{q\to q'}$, of the Morse oscillator for (a) $\lambda = 0.1$, (b) $\lambda = 1.0$, (c) $\lambda = 2.0$ and (d) $\lambda = 4.0$.

the Morse oscillator [18],

$$\phi_{n,q}(\xi) = \sqrt{\frac{\beta q!2(j-q)}{\Gamma(2j-q+1)}}\mathrm{e}^{-\xi/2}\xi^{j-q}L_q^{2(j-q)}(\xi+\sqrt{2}n\lambda l). \tag{7}$$

Here, $\xi = (2j+1)\exp(-\beta X)$ is the Morse coordinate, L the generalized Laguerre polynomial and Γ denotes the Gamma function. The total tunneling rate is $W^{n\to n'}_{q\to q'} = \sum_\alpha W^{n\to n'}_{q\to q',\alpha}$. In the sequential tunneling regime, the steady-state current is given by $I_\alpha = e\sum_{nqq'} P^n_q[W^{n\to n-1}_{q\to q',\alpha} - W^{n\to n+1}_{q\to q',\alpha}]$, where the bias voltage is $V = (\mu_\mathrm{L} - \mu_\mathrm{R})/e$.

3. Results

We will analyze the consequences of the model for both the Kondo temperature and the Coulomb blockade. In both cases, the important ingredients are the Franck–Condon matrix elements of the Morse potential. Corresponding numerical results are plotted in figure 1, which reveal two striking features: (i) the diagonal matrix elements decrease exponentially with increasing λ, whereas off-diagonal elements increase simultaneously, giving rise to the Franck–Condon blockade [20]; (ii) the Franck–Condon matrix is no longer symmetric under parity transformations. The direction of the relative shift of the potential surfaces of neutral and charged states, as determined by the sign of λ, is relevant for the overlap of two vibrational wavefunctions, and hence $M^{q\to q'}_{n\to n'} \neq M^{q'\to q}_{n\to n'}$ [18]. For a given sign of λ, the Franck–Condon elements $M^{q\to q'}_{n\to n'}$ with $q' < q$ are strongly suppressed in comparison with those with $q' > q$.

We first address the gate voltage dependence of the Kondo temperature within our model. Performing a Schrieffer–Wolff transformation [23] in the presence of anharmonic potential

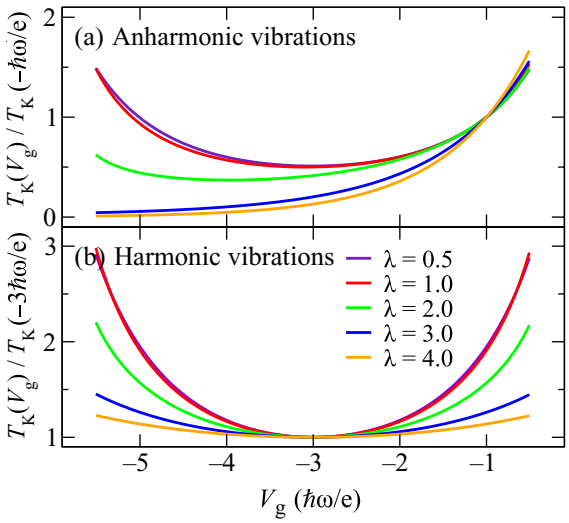

Figure 2. Kondo temperature as a function of gate voltage for (a) anharmonic and (b) harmonic vibrations. Here, we assume $U = 6\,\omega_0$, $\Gamma \equiv 2\pi\nu t^2 = \pi\omega_0$ and zero temperature.

surfaces, we obtain

$$J = 2t^2 \sum_{m=0}^{\infty} \left[\frac{|M_{0\to m}^{0\to 1}|^2}{\epsilon_d - \hbar\omega_0[m - \chi(m+1/2)^2 + \chi/4]} - \frac{|M_{0\to m}^{2\to 1}|^2}{\epsilon_d + U + \hbar\omega_0[m - \chi(m+1/2)^2 + \chi/4]} \right] \tag{8}$$

for the exchange coupling. Implications for the Kondo temperature as a function of gate voltage (setting $V_g = \epsilon_d$ for simplicity) are shown in figure 2(a) for different values of λ. Similar to the case of harmonic vibrations [17], which is presented in figure 2(b) for comparison, the gate-voltage dependence becomes weaker with increasing electron–vibron interaction λ. The origin of this suppression is that due to the Franck–Condon matrix elements $M_{0\to m}^{n\to n'}$, the dominant contribution to the exchange coupling in equation (8) for large λ stems from virtual charge fluctuations involving highly excited vibrational states with $m \approx \lambda^2$. Indeed, these states have maximal overlap $M_{0\to m}^{n\to n'}$ with the vibronic ground state. As a result, the energy denominators in equation (8) are dominated by the vibrational energy of the intermediate state, suppressing the dependence of the exchange coupling and consequently T_K on the gate voltage V_g.

The anharmonicity of the molecular potential surfaces results in an asymmetric dependence $T_K(V_g)$, which is most pronounced in the regime of strong electron–vibron coupling. For the symmetric case, the function $\ln T_K(V_g)$ is approximately a parabola, which can essentially be described by only taking into account the term with $q = \lambda^2$ in the expression for the exchange coupling in equation (8), i.e. $\ln T_K \propto (\epsilon_d - \hbar\omega_0\lambda^2)(\epsilon_d + U + \hbar\omega_0\lambda^2)/(U + 2\lambda^2\hbar\omega_0)$. For strong electron–vibron coupling, this parabola is flattened by increasing λ. In contrast, for the asymmetric case, the gate voltage dependence is approximately given by

$$\ln T_K \propto \frac{(\epsilon_d - \hbar\omega_0\lambda^2)(\epsilon_d + U + \hbar\omega_0\lambda^2)}{U + \alpha\lambda^2\hbar\omega_0 + \gamma\epsilon_d}, \tag{9}$$

in the regime of weak electron–vibron coupling, where $\alpha \equiv (M_{0\to 1}^{0\to\lambda^2} + M_{2\to 1}^{0\to\lambda^2})/M_{0\to 1}^{0\to\lambda^2}$ and $\gamma \equiv (M_{0\to 1}^{0\to\lambda^2} - M_{2\to 1}^{0\to\lambda^2})/M_{0\to 1}^{0\to\lambda^2}$, For stronger electron–vibron coupling, only one of the two

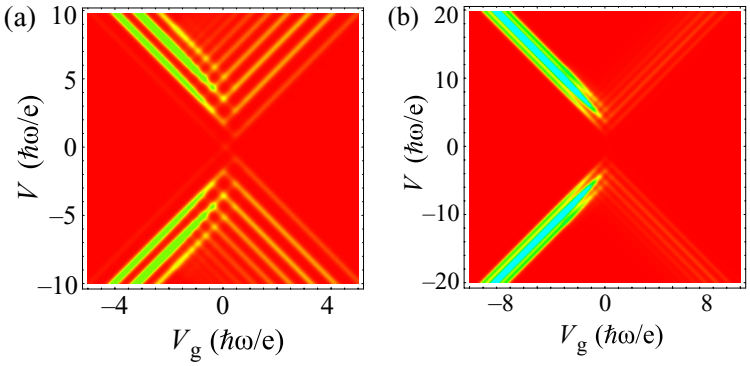

Figure 3. Differential conductance $\mathrm{d}I/\mathrm{d}V$ as a function of V and V_g for $\lambda = 2.0$, and temperatures (a) $T = 0.1\,\hbar\omega_0$ and (b) $T = 0.2\,\hbar\omega_0$.

energy denominators of the term with $q \approx \lambda^2$ in equation (8) is large, whereas the other one is negligible. Therefore, the parabolic gate voltage dependence $\ln T_\mathrm{K}(V_\mathrm{g})$ crosses over into a linear dependence, as can be seen from figure 2.

Next, we address the asymmetry in the Coulomb blockade peaks about the charge degeneracy point (marking the transition from the non-Kondo to the Kondo valley) which accompanies the quenching of the gate dependence of T_K in the experiment. To this end, we have computed the Coulomb blockade behavior in the presence of anharmonic vibronic potentials within the sequential tunneling approximation. (Of course, this approximation will not capture the Kondo physics at small biases.) Corresponding two-dimensional plots of the differential conductance as a function of bias voltage V and gate voltage V_g are shown in figure 3. We observe fine structure in the vicinity of the Coulomb blockade peaks (cf figure 3(a)) which results from excitations of bound states of the Morse oscillator, once the bias voltage exceeds the limits of the Coulomb blockade.

Interestingly, the number of visible peaks and the peak heights change drastically about the charge degeneracy point, where two molecular charge states become degenerate. While there occur only very few, but strongly pronounced peaks on one side, there are several consecutive weaker peaks on the other side.

The underlying physics behind this behavior is illustrated in figure 4. Due to the coupling of the electrons and the vibrations, the oscillator potential surfaces of the charged and uncharged states are shifted with respect to each other. As a consequence, the overlap of two wave functions with occupancy differing by unity depends strongly on their vibrational quantum numbers.

If the neutral state is energetically *below* the singly charged one (as shown in figure 4(a)), the spatial overlap of the state with $n = 0$, $q = 0$ and several states with charge $n = 1$ and higher vibronic states are of the same order of magnitude. The wavefunctions assume large values in the vicinity of the classical turning points. Since the position of the *left* turning point is similar for a large number of vibronic states, the corresponding inelastic transition rates involving the excitation of vibrons are comparatively large likewise.

On the other hand, if the neutral state is energetically *above* the singly charged state (cf 4(b)), the situation looks qualitatively different. Only the spatial overlaps of the vibronic ground state with $n = 0$, $q = 0$ and very few excited vibronic states with $n = 1$ are significant. Since the position of the right turning point changes drastically as a function of the vibrational quantum number, there are only very few Franck–Condon matrix elements which are of

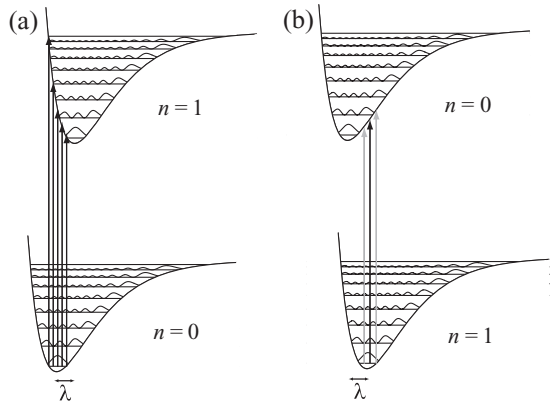

Figure 4. Level schemes showing the relevant vibrational excitations for a ground state with occupancy (a) $n = 0$ and (b) $n = 1$.

the same order of magnitude, so that the number of peaks in $\mathrm{d}I/\mathrm{d}V$ is small, whereas the corresponding peak heights are large.

We note in passing that the saturation value of the current does not depend on the gate voltage, so that the sum of all differential-conductance peak heights is equal for both sides of the degeneracy point.

Our crucial observation with regard to the experimentally observed asymmetry of the Coulomb blockade peaks involves the effect of thermal broadening at finite temperature. As shown in figure 3(b), thermal broadening washes out the fine structure with the characteristic temperature scale given by the vibrational frequency $\hbar\omega_0$ (with a rather small numerical prefactor). Due to the asymmetry in the number and strength of vibrational sidebands on both sides of the charge degeneracy point, this induces a pronounced asymmetry of the Coulomb blockade which is quite reminiscent of the experimental data. In fact, due to the thermal broadening, the closely spaced peaks on one side of the charge degeneracy point effectively merge into one peak, while the more widely spaced peaks on the other side are merely suppressed. We want to emphasize that this feature is characteristic of the regime of the strong (and intermediate) electron–vibron interaction, whereas it disappears entirely in the weak coupling limit.

4. Summary and conclusions

In summary, we have analyzed the effects of anharmonic potential surfaces on Coulomb blockade and Kondo physics in single-molecule transistors. Our study was motivated by recent measurements for single-molecule devices which have reported the simultaneous occurrence of two striking features: firstly, the observed gate-voltage dependence of the Kondo temperature is much weaker in comparison with quantum dots. Secondly, the differential conductance reveals peaks with drastically different intensities at the two opposite sides of the charge degeneracy point. We argue that strong electron–vibron coupling which favors anharmonic potential surfaces can explain both observations within a single generic model.

Our explanation is an alternative to previous suggestions, also relying on strong electron–vibron coupling, but relating the asymmetry in the Coulomb blockade to the influence of Kondo correlations. Possible experimental signatures which can distinguish between the two explanations include: (i) anharmonic potential surfaces should lead to a nonparabolic dependence of the Kondo temperature on gate voltage; (ii) in our model, the suppressed Coulomb blockade peaks can in principle occur on either side of the charge degeneracy point, dependent on the specific molecule under consideration and independent of whether one is concerned with a Kondo or non-Kondo valley. We hope that future experiments will investigate these issues.

Acknowledgments

We thank J Koch, D Natelson, J Paaske and M E Raikh for valuable discussions. Support by the DFG through Sfb 658 and Spp 1243 is gratefully acknowledged. This work has also been supported in part by DIP.

References

[1] Glazman L I and Raikh M E 1988 *JETP Lett.* **47** 452
[2] Ng T K and Lee P A 1988 *Phys. Rev. Lett.* **61** 1768
[3] Goldhaber-Gordon D, Shtrikman H, Mahalu D, Abusch-Magder D, Meirav U and Kastner M A 1998 *Nature* **391** 156
[4] Cronenwett S M, Oosterkamp T H and Kouwenhoven L P 1998 *Science* **281** 540
[5] van der Wiel W G, De Franceschi S, Fujisawa T, Elzerman J M, Tarucha S and Kouwenhoven L P 2000 *Science* **289** 2105
[6] Sela E *et al* 2006 *Phys. Rev. Lett.* **97** 060501
[7] Paaske J and Flensberg K 2005 *Phys. Rev. Lett.* **94** 176801
[8] Galperin M, Nitzan A and Ratner M A 2007 *Preprint* 0705.2217
[9] Glazman L I and Pustilnik M 2005 Low-temperature transport through a quantum dot *Nanophysics: Coherence and Transport* (Amsterdam: Elsevier) pp 427–78
[10] Rosch A, Kroha J and Wölfle P 2001 *Phys. Rev. Lett.* **87** 156802
Paaske J, Rosch A, Kroha J and Wölfle P 2004 *Phys. Rev.* B **70** 155301
[11] Coleman P, Hooley C and Parcollet O 2001 *Phys. Rev. Lett.* **86** 4088
[12] Kaminski A, Nazarov Y V and Glazman L I 2000 *Phys. Rev.* B **62** 8154
[13] Yu L H, Keane Z K, Ciszek J W, Cheng L, Tour J M, Baruah T, Pederson M R and Natelson D 2005 *Phys. Rev. Lett.* **95** 256803
[14] Liang W *et al* 2002 *Nature* **417** 725
[15] Yu L H and Natelson D 2004 *Nano Lett.* **4** 79
[16] Yu L H *et al* 2004 *Phys. Rev. Lett.* **93** 266802
[17] Balseiro C A, Cornaglia P S and Grempel D R 2006 *Phys. Rev.* B **74** 235409
Cornaglia P S, Usaj G and Balseiro C A 2007 *Phys. Rev.* B **76** 241403
[18] Morse P M 1929 *Phys. Rev.* **34** 57
[19] Mitra A, Aleiner I and Millis A J 2004 *Phys. Rev.* B **69** 245302
[20] Koch J and von Oppen F 2005 *Phys. Rev. Lett.* **94** 206804
[21] Galperin M, Ratner M A and Nitzan A 2006 *Preprint* cond-mat/0612085
[22] Koch J and von Oppen F 2005 *Phys. Rev.* B **72** 113308
[23] Schrieffer J R and Wolff P A 1966 *Phys. Rev.* **149** 491